Med Biol Eng Comput
DOI 10.1007/s11517-008-0403-2

SPECIAL ISSUE - ORIGINAL ARTICLE

"Wave" as defined by wave intensity analysis

Jiun-Jr Wang · Nigel G. Shrive · Kim H. Parker · John V. Tyberg

Received: 7 April 2008 / Accepted: 19 September 2008

Abstract The propagation of waves in the arteries is generally described using Fourier analysis in terms of periodic wavetrains formed by the superposition of a mean value and sinusoidal waves at the fundamental frequency (defined by the heart rate) and its harmonics. There is, however, an alternative way to describe waves in the vasculature based upon the method-of-characteristics solution of 1-D conservation laws. This method, wave intensity analysis (WIA), can be used to describe periodic waves but can also be used to describe the propagation of non-periodic waves that cannot be practically described in terms of sinusoidal wavetrains. As a means of demonstrating how WIA defines a wave, we used data gathered in a simple bench-top experiment where a single disturbance propagated along a single elastic tube and was reflected and re-reflected between a closed and a relatively open end. Results demonstrate that forward- and backward-travelling peaks of intensity usefully define wave interactions.

J.-J. Wang · N. G. Shrive · K. H. Parker · J. V. Tyberg
Department of Cardiac Sciences,
Libin Cardiovascular Institute of Alberta,
University of Calgary, Calgary, Canada

J.-J. Wang (✉)
Department of Physiology and Biophysics,
Health Sciences Centre, Libin Cardiovascular Institute
of Alberta, University of Calgary, 3330 Hospital Dr. NW,
Calgary, AB T2N 4N1, Canada
e-mail: jjwang@ucalgary.ca

N. G. Shrive
Department of Civil Engineering, University of Calgary,
Calgary, Canada

K. H. Parker
Department of Bioengineering, Imperial College of Science,
Technology and Medicine, London, UK

Keywords Non-periodic wave · Benchtop · Repeated reflections

1 Introduction

Womersley was perhaps the most important figure in the development of modern arterial hemodynamics. His famous 1958 work [14] on the velocity profile of pulsatile blood flow turned the study of arterial hemodynamics overwhelmingly in favor of frequency-domain Fourier analysis. In this approach, periodic aortic pressure and flow waveforms are understood to be the summation of a mean value plus superimposed sinusoidal wavetrains at the fundamental frequency (i.e., the heart rate) and at its harmonics. The paper by O'Rourke in this Special Issue summarizes the accomplishments achieved by this approach [6].

Two decades ago Parker and Jones developed an alternative time-domain approach, wave intensity analysis (WIA), which was derived using the method of characteristics and was intended to identify the type (compression or decompression waves; decompression waves were previously termed expansion waves), magnitude and direction of local waves [8]. Each cardiac cycle is considered to be independent so there is no restriction on the periodicity of the data to be analyzed. WIA has been applied to the study of aortic hemodynamics, the coronary [11] and pulmonary circulations [1, 2], and LV [13] and RV [10] ventricular diastolic function.

A "wave", defined as a propagating disturbance [4, 7], can be generated by harmonic motions (sound waves, water surface waves etc.), which can be described naturally using Fourier analyses. The character of a sinusoidal wave is that in each harmonic, energy is transmitted

without transportation of mass. A wave can also be generated by non-periodic displacements. Tsunamis in the ocean and bores in estuaries are just two examples in which both the energy and mass are transported. These waves were solitary and non-periodic in nature and they may not be easily described in terms of sinusoidal wavetrains. Methods have been developed in gas and fluid dynamics to treat these non-periodic waves conceptually and analytically.

To create a wave in a simple, controlled system and to demonstrate our interpretation, we performed a bench-top experiment on a homogeneous elastic tube, with the distal end closed and the proximal end essentially open to atmospheric pressure. Simultaneous pressure and flow measurements were taken at ten sites along the tube. A solitary decompression wave was generated at the inlet, which allowed us to investigate the propagation and reflection of a single disturbance, without interference from succeeding disturbances. Using WIA, the propagation of the decompression wave could be observed clearly; it was reflected and re-reflected between the distal closed-end and the proximal open-end reflection sites. This process could be followed for three or more cycles before the wave dissipated.

2 Methods

2.1 Apparatus

An elastic tube (2-m long, 19.0 mm in outside diameter and 3.18 mm wall thickness; Tygon, Saint-Gobain Plastics, Akron, OH) was connected to a balloon contained in a closed glass bottle (see Fig. 1). The distal end of the tube was closed with a rubber stopper and the balloon and tube were filled with degassed water. The stopper of the bottle was penetrated by a T-shaped connector, one leg of which was connected to a syringe and the other was open to the atmosphere. Pressures were measured using catheter-tip transducers (Millar Instruments Inc., Houston, TX) and flow, using an ultrasonic flowmeter (Transonic Systems, Ithaca, NY). A decompression wave (we found compression waves more difficult to generate reproducibly and reliably) was generated repeatedly; pressure was measured in the balloon as a reference and pressure and flow were simultaneously measured at ten different locations along the tube, sequentially, starting from the proximal end. This enabled us to plot pressure, flow, and wave intensity versus time and distance.

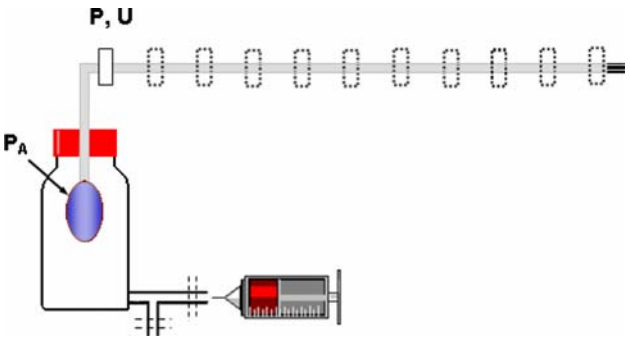

Fig. 1 Diagram of the bench-top apparatus. P_B, pressure measured inside the balloon; P and Q, simultaneously measured pressure and flow. The dashed rectangles indicate the locations of the measurements of P and Q

First, we closed the open end of the T-connector with a surgical clamp and pressurized the bottle to 40 mmHg. When the clamp was released quickly, the bottle was depressurized to atmospheric pressure to generate a decompression wave and the ensuing pressure and flow changes were recorded. After the waves had dissipated, the pressure and flow transducers were moved by 20-cm increments from the open end of the tube to the closed end. After each move, the decompression wave was regenerated and measurements were taken.

2.2 Data analysis

Paired pressure and velocity (calculated from flow) data were used to calculate the intensities of forward- and backward-travelling waves where 'forward' refers to travel away from the balloon. 3-D plots of pressure and flow against time and distance were constructed by taking the proximal balloon pressure as the temporal reference and aligning the balloon pressure of each measurement accordingly. The temporal reference value, $t = 0$, was arbitrarily chosen as 10 ms before the onset of the pressure drop inside the balloon. The superposition of balloon-pressure changes between different runs demonstrated that reproducibility was excellent.

Wave speed was evaluated using the foot-to-foot method.

The reflections at the ends of the tube was characterised by a reflection index calculated as the ratio of the reflected to the incident intensity.

3 Results

Releasing the clamp caused balloon pressure to fall quickly and exponentially to atmospheric pressure ($\tau = 13.0 \pm 0.1$ ms; 95% of the pressure decrease [i.e., to a level of 2 mmHg] was achieved in 59.8 ± 0.4 ms).

Wave speed was found to be 25.3 ± 0.2 m/s.

Pressure (Fig. 2a) and flow (Fig. 2c), measured at 20-cm intervals along the tube, are plotted against time and

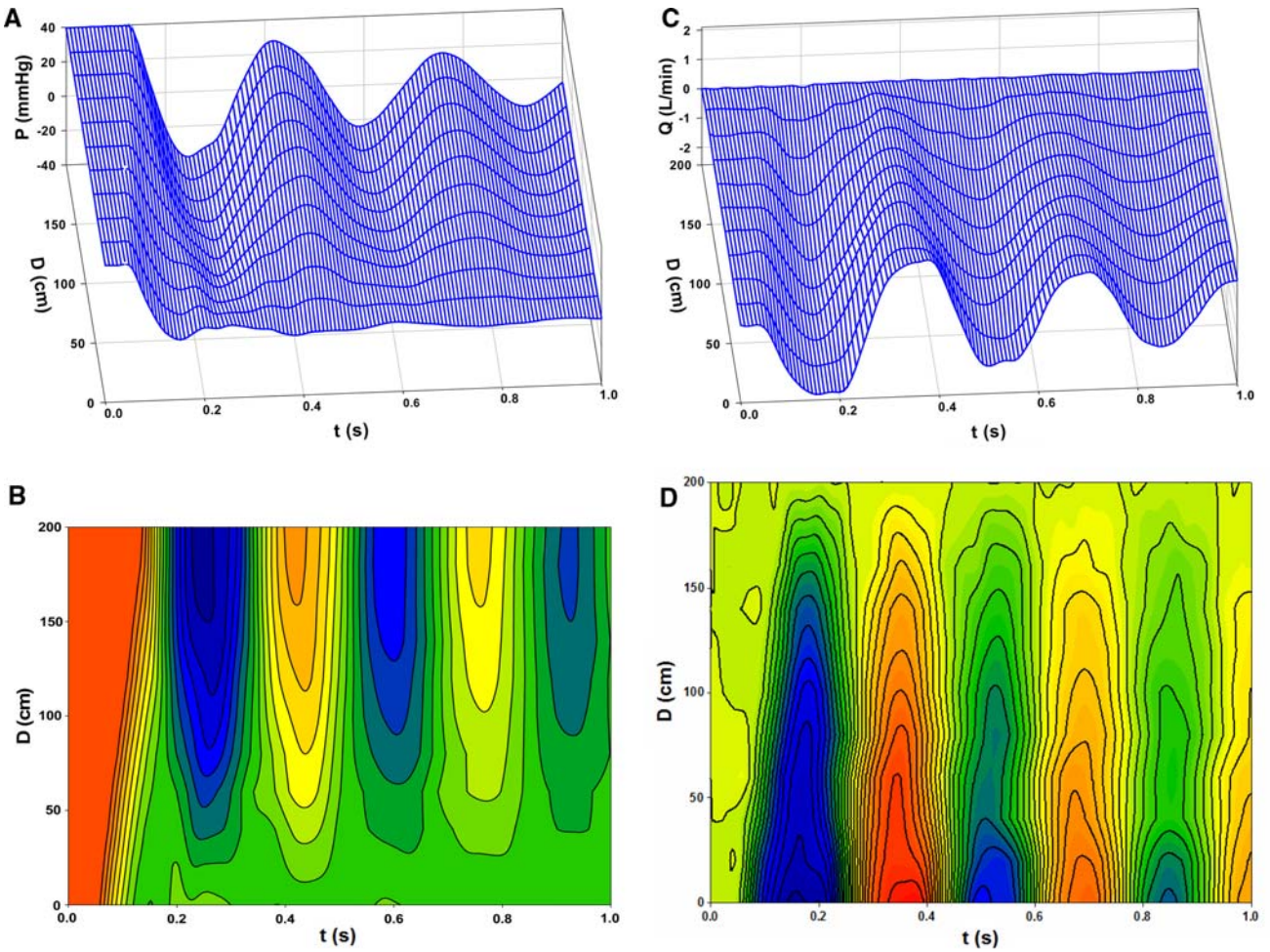

Fig. 2 **a** Pressure plotted as a function of time (t) and distance (D) in the bench-top experiment. **b** Flow plotted as a function of t and D

distance. The patterns of recorded pressure and flow are distinctly different. Upon depressurization, the decompression wave induced a decrease in pressure and backward flow (i.e., toward the balloon). At the proximal end ($D = 0$ cm) that was opened to atmospheric pressure, pressure variations were minimal but flow variations were maximal; at the distal end ($D = 200$ cm) that was closed with a stopper, pressure variations were maximal but flow variations were minimal.

Using wave-intensity analysis, the forward and backward waves were defined and plotted versus time and distance in Fig. 3a, b, respectively. The forward decompression wave (FDW) generated by the deflation of the balloon propagated along the tube and was reflected by the distal closed end as a backward decompression wave (BDW) which, in turn, was reflected negatively by the proximal open end as a forward compression wave (FCW). From the closed end, it was again reflected as a backward compression wave (BCW). These patterns were repeated until the wave dissipated.

The reflection index at the distal (closed) end was found to be 1.0 ± 0.0 and that at the proximal (effectively open) end, -0.97 ± 0.03.

Figure 4 illustrates how we defined the spatial and temporal extents of the wave. First, the time ($t = 0.111$ s; red line) at which the peak of the FDW had arrived at the mid-point of the tube ($D = 100$ cm; black line) was identified. Figure 4a shows a detailed contour plot of the FDW shown in Fig. 3a. The contour lines represent 10% differences from the peak value of wave intensity at $D = 100$ cm and $t = 0.111$ s. The intersections of the contour lines with the $D = 100$ cm and $t = 0.111$ s lines are identified by black and red dots, respectively. Next, the spatial extent of the wave at that time was evaluated by identifying the points at which wave intensity was equal to half its maximal value. As indicated by the red arrow, the distance between the half-maximum wave intensity points at $t = 0.111$ s was taken as the wave length parameter, $\lambda_{0.5}$, which equals 110 cm in this example. This measure of the spatial extent of the wave was chosen because the foot

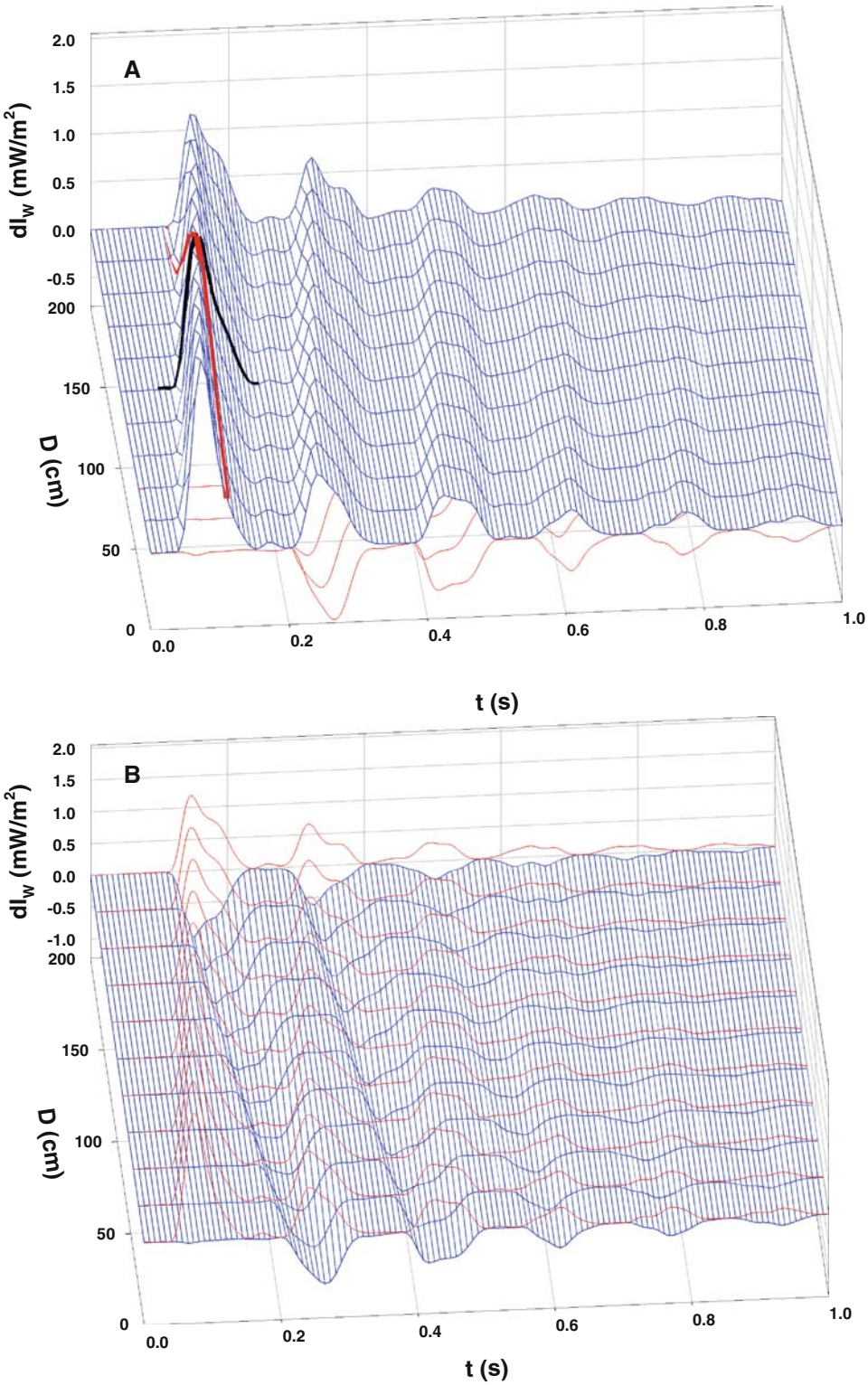

Fig. 3 Separated wave intensity. **a** Wave intensity of forward-going waves (*Black* and *red orthogonal lines* refer to Fig. 4). **b** Wave intensity of the backward-going waves (color available only in online version)

of the wave and, hence, the total extent of the wave was difficult to determine exactly. In a similar way, it is possible to define the temporal extent of the wave. The black arrow, which indicates the interval between the half-maximum wave intensity points at $D = 100$ cm, was taken as the temporal, wave duration parameter, $\Delta t_{0.5} = 0.045$ s. In Fig. 4b, the values of the FDW at the maximum, 90, 80, 70, 60, and 50% of the maximum values are identified with black and red dots and the contours of the wave at that time and distance are drawn. These values characterize the

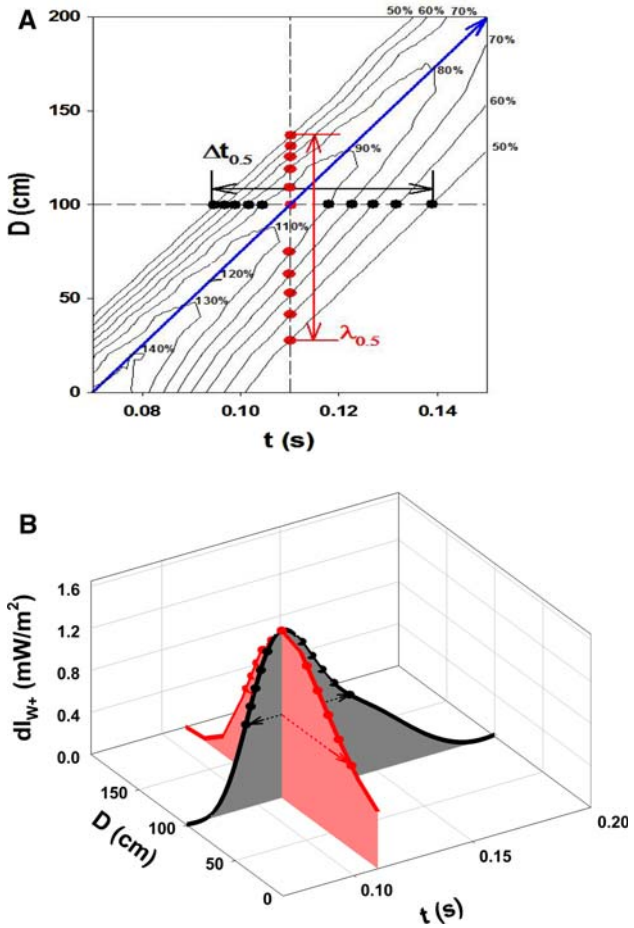

Fig. 4 **a** Detailed contour plot of the forward-going decompression wave (*FDW*) as a function of distance (*D*) and time (*t*), corresponding to Fig. 3a. *Contour lines* represent 10% differences from the maximum value of intensity (i.e., 1.6 mW/m^2) at the intersection of the *black* ($D = 100$ cm) and *red* ($t = 0.111$ s) *lines*. The *red, double-headed arrow* indicates $\lambda_{0.5}$. The *black, double-headed arrow* indicates $\Delta t_{0.5}$. The *blue dashed arrow* indicates the distance-time progression of the peak of the FDW. **b** 3-D plot of the intensity of the FDW at $D = 100$ cm (*black*) and $t = 0.111$ s (*red*). *Red* and *black* points respectively represent 90, 80, 70, 60, and 50% of the maximum-intensity values in time and distance. See text (color available only in online version)

spatial and temporal extents of the wave at $D = 100$ cm and $t = 0.111$ s.

4 Discussion

For the past fifty years, aortic pressure and flow have been analyzed predominately by Fourier-based methods. WIA provides an alternative way of looking at arterial waves, which is based upon the method of characteristics solution for hyperbolic equations introduced by Riemann [9], which has been developed extensively in the study of compressible gas dynamics. The mathematical analysis may appear complex, but the results are surprisingly simple. Any disturbance (i.e., the change in pressure, dP, and velocity, dU) generated at the root of a homogeneous tube will propagate unchanged downstream with the speed $U + c$, where U is the instantaneous velocity and c is the wave speed. This wave propagates unchanged until it encounters a change in the properties of the vessel (e.g., a change in area or in distensibility) where a reflected and a transmitted wave will be generated. The reflected wave will propagate unchanged upstream toward the origin of the tube with the speed $U - c$. Thus, waves travel forward and backwards with the local wave speed $\pm c$ but are convected with the blood velocity, U. The power per unit area (W/m^2) of the disturbance is defined as the net intensity, d$P \times$ dU. With assumptions of superposition, the net intensity can be separated into the forward-, $(4\rho c)^{-1}$ $(\mathrm{d}P + \rho c\ \mathrm{d}U)^2$, and backward-traveling components, $-(4\rho c)^{-1}(\mathrm{d}P - \rho c\ \mathrm{d}U)^2$ (7).

In contrast to previous studies [3, 5, 12], where periodic waveforms were the input to the system, we used a single disturbance and the sole purpose of this paper has been to provide a clear and direct explanation and demonstration of how WIA defines a wave. This seemed to be necessary and important because, explicitly or implicitly, "wave" has been given several different definitions in the literature of arterial hemodynamics. First, wave sometimes means a peak in a pressure or flow waveform. Second, wave often refers to a sinusoidal oscillation at the fundamental frequency (i.e., the heart rate) and/or at a harmonic (i.e., a multiple) of that frequency. Finally, wave has been applied to the theoretical components of diastolic pressure or flow which, when added together, equal the measured diastolic pressure or (zero) diastolic flow.

As we have demonstrated here, WIA defines how the wave travels in distance and time. In addition, WIA shows how, at any location, the wave is distributed in time and, at any instant of time, it is distributed in distance. Because, in distance and time, the "edges" of the wave approach zero asymptotically, the onset and offset of the wave are very difficult to define. Therefore, we have characterized the spatial and temporal extents of the wave in terms of the distance and the interval spanned by the wave at a higher level where definition is unequivocal, arbitrarily at 50% of its maximum intensity as is common in other fields such as spectroscopy and chromatography where peaks are regularly encountered.

The concept of a temporal "wave width" might be understood more easily with the aid of a simple analogy. Imagine standing of the side of a road, looking directly across the road. A truck passes. The length of the truck is $\lambda_{0.5}$, and the length of time it takes to pass is $\Delta t_{0.5}$. In the context of Fig. 4b, if one were standing at the 100-cm point, the nose of the truck would pass at the first black dot (the one furthest to the left), the truck would pass in time as

the black dots progress to the right, and the tail of the truck would pass the observer at the black dot furthest to the right. The length of the truck is shown by the line of red dots.

The shape of the wave is a function of the time course of the initial perturbation. In this bench-top experiment, opening the bottle to atmospheric pressure caused balloon pressure to fall with a τ of 13 ms. In comparison, LV relaxation is characterized by values of τ of the order of 45 ms so the value of dP is greater than that in the aorta during relaxation. Because wave intensity is a function of dU as well as dP, the shape is also a function of the inertia of the column of liquid because intensity is determined by acceleration. The inertia of the bench-top system might be greater than that of the aorta at the aortic valve because the column is 2 m long and the plastic tubing, relatively stiff. Thus, wave intensity might be greater than physiologic values. However, it was not the goal of this study to simulate LV relaxation quantitatively, only to demonstrate the properties of a reproducibly generated wave.

The wave was reflected from the closed end with a reflection index of 1.0 (since $dU = 0$ at the distal end). It was reflected from the proximal, open end with a reflection index of -0.97 ± 0.03, consistent with a substantial area expansion of somewhat greater than ten times [7]. This essentially open-end behavior caused compression waves to be reflected as decompression waves and vice versa.

The advantages of WIA can be demonstrated from the results of our well-controlled, bench-top experiment. Although the patterns of pressure and flow changes are regular (Fig. 2), wave motion is difficult to discern from either the pressure or flow waveform alone. Because the far end of the tube was closed and the near end was essentially open, pressure variations were maximal at the far end and flow variations were maximal at the near end. The use of WIA to identify the forward and backward waves provides a definitive, physically coherent representation of wave propagation (Fig. 3). Several reflections and re-reflections are obvious and the energy of the wave is well-conserved, consistent with a plausible degree of dissipation and distortion.

5 Conclusion

The results of the bench-top experiment show that WIA can be useful in the interpretation of non-periodic waves in elastic vessels. In the absence of periodicity, it is impossible to use the wave length defined as the distance between crests or troughs of the wave to describe a solitary wave. We suggest that the distance between the 'half-heights' of the wave intensity can be used to characterise the extent of a solitary wave. Similarly, in the absence of a 'period', we suggest that the time between the 'half-heights' of the wave intensity can be used to characterise its duration.

In this experiment, we did not intend to duplicate arterial conditions, but to produce a solitary wave that could be repeated reproducibly. Because compression induced unwanted oscillations in the balloon attached to the tube, we used decompression to generate the waves. Similarly, no attempt was made to reproduce the magnitude and duration of aortic disturbances in the experiment.

Despite this, the results of the experiment do have implications for the understanding of aortic waves in vivo. They show that there is an alternative way of describing aortic waves that does not rely upon them being periodic, but can be used equally well when the waves are periodic. They also show that wave intensity can be useful for understanding the effects of reflections in the aorta. It provides information about the direction and magnitude of the waves that can be helpful in interpreting the complex pattern of reflections that make up the observed pressure and velocity waveforms measured in vivo.

References

1. Hollander EH, Dobson GM, Wang JJ, Parker KH, Tyberg JV (2004) Direct and series transmission of left atrial pressure perturbations to the pulmonary artery: a study using wave-intensity analysis. Am J Physiol Heart Circ Physiol 286:H267–H275. doi:10.1152/ajpheart.00505.2002
2. Hollander EH, Wang JJ, Dobson GM, Parker KH, Tyberg JV (2001) Negative wave reflections in pulmonary arteries. Am J Physiol Heart Circ Physiol 281:H895–H902
3. Kenner T, Wetterer E (1967) Experimental studies on a tube model of impedance continuously increased toward the periphery. Pflugers Arch Gesamte Physiol Menschen Tiere 295:99–118. doi:10.1007/BF00362742
4. Lighthill MJ (1959) Introduction to Fourier analysis and generalised functions. Cambridge University Press, Cambridge
5. Newman DL, Masters NJ, McNulty JF (1975) Pulse-wave reflection in elastic tubes. Med Biol Eng 13:720–726. doi:10.1007/BF02477333
6. O'Rourke MF Clinical applications of impedance analysis. Med Biol Eng Comput 1:1, 8 A.D.
7. Parker KH (2008) An itroduction to wave intensity analysis. http://www.bg.ic.ac.uk/research/intro_to_wia/welcome.html
8. Parker KH, Jones CJH (1990) Forward and backward running waves in the arteries: analysis using the method of characteristics. J Biomech Eng 112:322–326. doi:10.1115/1.2891191
9. Riemann G (1953) The Collected Works of Bernhard Riemann. Dover, New York
10. Sun Y, Belenkie I, Wang JJ, Tyberg JV (2006) Assessment of right ventricular diastolic suction in dogs with the use of wave intensity analysis. Am J Physiol Heart Circ Physiol 291:H3114–H3121.doi:10.1152/ajpheart.00853.2005
11. Sun Y-H, Anderson TJ, Parker KH, Tyberg JV (2000) Wave-intensity analysis: a new approach to coronary dynamics. J Appl Physiol 89:1636–1644
12. Taylor MG (1959) An experimental determination of the propagation of fluid oscillations in a tube with a visco-elastic wall;

together with an analysis of the characteristics required in an electrical analogue. Phys Med Biol 4:63–82. doi:10.1088/0031-9155/4/1/308

13. Wang Z, Jalali F, Sun YH, Wang JJ, Parker KH, Tyberg JV (2005) Assessment of left ventricular diastolic suction in dogs using wave-intensity analysis. Am J Physiol Heart Circ Physiol 288:H1641–H1651. doi:10.1152/ajpheart.00181.2004
14. Womersley JR (1958) Oscillatory flow in arteries: the reflection of the pulse wave at junctions and rigid inserts in the arterial system. Phys Med Biol 2:178–187. doi:10.1088/0031-9155/2/2/305